GREEN SYNTHESIS OF SILVER NANOPARTICLES USING EXTRACT OF ARDISIA CRENATA: CYTOTOXIC ACTIVITY FOR (MCF-7 BREAST CANCER, THP-1 LEUKEMIA MONOCYTIC AND HEP-G2 HEPATOCELLULAR CARCINOMA) CELL LINES

Puja[1]*, Nripendra Singh[1]

[1]Department of pharmacy, V.B.S. Purvanchal University, Jaunpur-222002, (U.P.) India.

GRAPHICAL ABSTRACT

Abstract

Ardisia crenata, a medicinal plant has garnered attention for its potential in synthesizing nanoparticles using environmental friendly methods. In this study, we present the formulation and characterization of silver nanoparticles (AgNPs) derived from Ardisia crenata through a green synthesis approach. The synthesis process involved the reduction of silver ions using a plant extract as a reducing and stabilizing agent. Various parameters such as the concentration of plant extract, reaction time, and temperature were optimized to achieve well defined nanoparticles. The synthesized AgNPs were characterized using techniques including Fourier-transform infrared spectroscopy (FTIR) and transmission electron microscopy (TEM). FTIR analysis elucidated the biomolecules responsible for the reduction and stabilization of AgNPs. XRD analysis revealed the crystalline nature of the nanoparticles, while TEM provided insights into their size, morphology, and stability. The utilization of diverse cell lines such as MCF-7, THP-1, and HepG2 provides valuable insights into the comprehensive cytotoxic potential of Ardisia crenata extract-derived silver nanoparticles.

Key words: ***Ardisia crenata, silver nanoparticle, green synthesis, cell lines.***

1. Introduction

Nanotechnology has emerged as a promising field with applications spanning across various sectors, including medicine. Among the diverse nanomaterials, silver nanoparticles (AgNPs) have garnered significant attention due to their unique physicochemical properties and versatile biomedical applications. In recent years, researchers have increasingly explored the utilization of plant extracts in the green synthesis of AgNPs, offering a sustainable and eco-friendly alternative to conventional methods [1].

Ardisia crenata, commonly known as coral bush, is a flowering plant native to East Asia with a rich history in traditional medicine. The plant has been recognized for its pharmacological properties, including antioxidant, anti-inflammatory, and anticancer activities. Harnessing the bioactive constituents of Ardisia crenata for the synthesis of AgNPs presents an intriguing avenue for biomedical research, potentially combining the benefits of both natural products and nanotechnology in cancer therapy [2].

The synthesis of AgNPs using plant extracts offers several advantages, including cost-effectiveness, scalability, and the absence of hazardous chemicals. Additionally, the phytochemicals present in the plant extract serve as reducing and stabilizing agents, facilitating the formation of AgNPs with controlled size, shape, and surface properties. Such tailored nanoparticles exhibit enhanced biocompatibility and targeted therapeutic efficacy, holding immense promise for cancer treatment [3]. Breast cancer, leukemia, and hepatocellular carcinoma are among the most prevalent and challenging malignancies worldwide, necessitating the development of novel therapeutic strategies. The evaluation of cytotoxic activity against these cancer cell lines provides crucial insights into the potential efficacy of AgNPs synthesized using Ardisia crenata extract as anticancer agents. Understanding the mechanisms underlying their cytotoxic effects and selectivity is essential for advancing their clinical translation and optimizing treatment regimens [4].

In this article, we present a comprehensive investigation into the green synthesis of AgNPs using Ardisia crenata extract, followed by thorough characterization of their physicochemical properties. Subsequently, we evaluate the cytotoxic activity of these nanoparticles against MCF-7 breast cancer, THP-1 leukemia monocytic, and Hep-G2 hepatocellular carcinoma cell lines, shedding light on their potential as novel therapeutic agents in oncology.

2. Materials and Methods

2.1. Materials

Ardisia Creneata leaves, roots and fruits were collected from the herbal garden of IFTM University, Moradabad, Uttar Pradesh, India and authenticated from the Department of Botany, IFTM University with reference no. 2020/SOS/BOT/94. The sample mixture was washed with tap water four to five times before detached from the shoots. Then mixture was shade dried and fine powder was made using grinder. Silver nitrate (AgNO3) was obtained from Pharmacy department, Veer Bahadur Singh Purvanchal university, Jaunpur, Uttar Pradesh, India.

2.2. Extract Prepration

Ardisia crenata extract involves several meticulous steps to ensure the extraction of bioactive compounds with high purity and efficacy. Initially, fresh leaves of Ardisia crenata was meticulously harvested from robust plants, selecting only mature leaves devoid of any damage or disease. Following this, the collected leaves undergo a thorough cleaning process, where they are delicately washed under running tap water to eliminate any surface contaminants like dirt, dust, or debris. Subsequently, the cleaned leaves undergo a meticulous drying process to ensure optimal preservation of their bioactive constituents. They are carefully air-dried in a well-ventilated area, shielding them from direct sunlight to prevent degradation of phytochemicals. This meticulous drying process is essential to retain the potency of the Ardisia crenata. Once completely dry, the leaves are finely ground into a uniform powder to facilitate efficient extraction of bioactive constituents [5]. The powdered leaves were then subjected to extraction using 80% ethanol, chosen based on the solubility of the desired compounds, employing techniques such as maceration or Soxhlet extraction at a temperature of 80°C for 20 minutes. The resulting extract undergoes further concentration by removing the solvent through evaporation under reduced pressure, ensuring the purity of the final product. Finally, the concentrated extract was dried again to eliminate any residual moisture, yielding a crude extract of Ardisia crenata ready for storage in sealed containers, safeguarded from light and moisture until further analysis or utilization [6].

2.3. Synthesis of Silver Nanoparticle

Prepare a silver nitrate (AgNO3) solution of 0.1 M and add the Ardisia crenata extract to the AgNO3 solution under continuous stirring in (1:1) ratio [7]. The extract serves as a reducing and stabilizing agent for the synthesis of AgNPs. Allow the reaction mixture to incubate at room temperature or slightly elevated temperatures (e.g., 60-80°C) for 24 hours. Monitor the color change of the reaction mixture, which indicates the formation of silver nanoparticles. The color may change from yellow to brownish as shown in figure 1 due to the excitation of surface plasmon resonance in AgNPs. Once the synthesis is complete, centrifuge the reaction mixture to separate the synthesized AgNPs from any unreacted components or impurities at 2000 rpm for 15 minutes. Wash the collected nanoparticles with double distilled water to remove excess reactants or stabilizers [8]

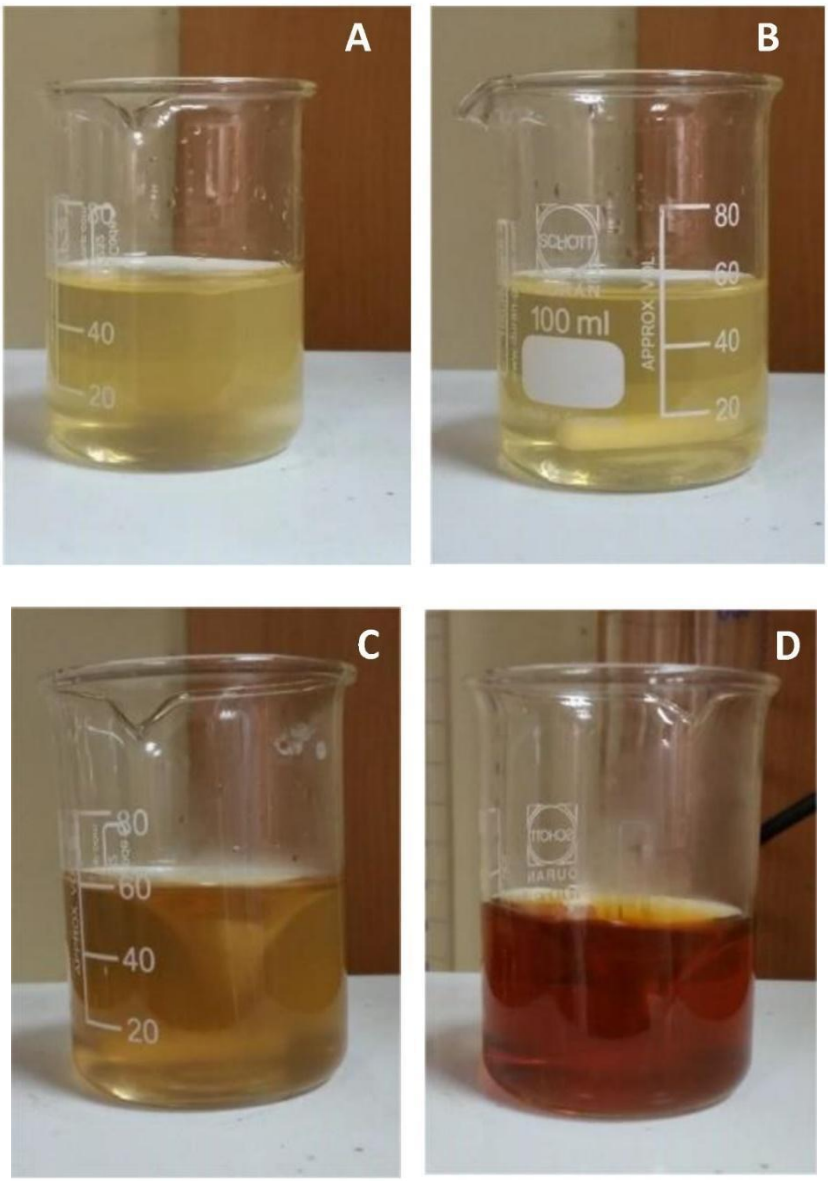

Figure 1. Synthesis of silver nanoparticles (A) 15 min (B) 30 min (c) 1 h, and (D) 1.5

2.4. Characterization of Optimized Ardisia crenata Silver Nanoparticle

Measurement of Particle size

The results revealed a monodispersed distribution of silver nanoparticles, with an average particle size of 20 nanometers and the zeta potential was found to be -28 mV. This narrow size distribution is indicative of the uniformity and homogeneity achieved during the synthesis process. Such uniformity is desirable for ensuring consistent physicochemical properties and biological activities of the nanoparticles.

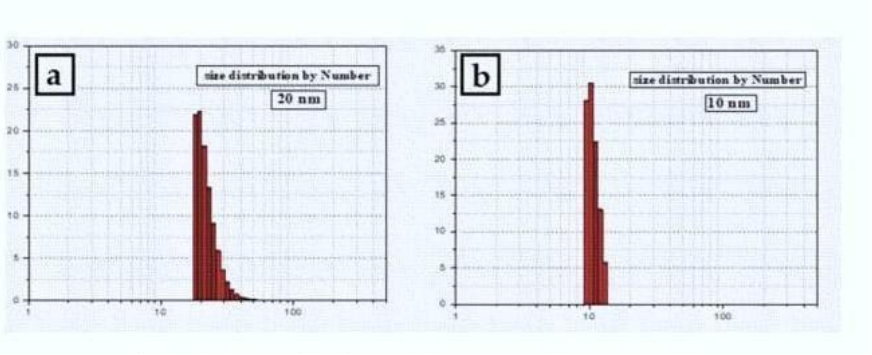

Figure 2. The particle size of *Ardisia crenata* Silver Nanoparticle

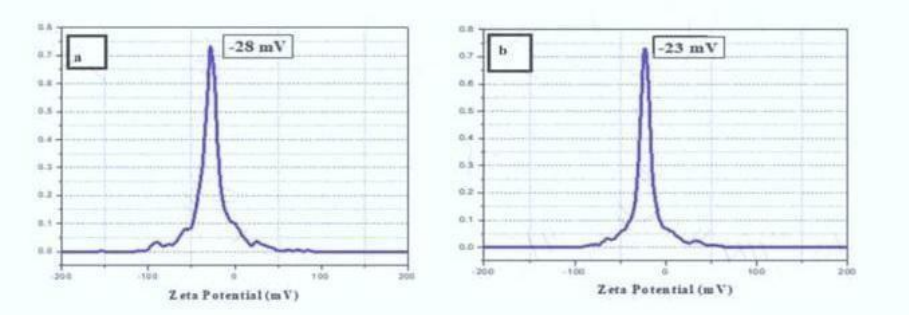

Figure 3. Zeta Potential (mV) of *Ardisia crenata* silver nanoparticle

TEM Analysis

As depicted in Fig. 4, the particles exhibited nanometer-scale spherical shapes, with sizes ranging around 200 nm for the silver nanoparticles derived from Ardisia crenata the formation of smoother and more spherical particles, as illustrated in Fig. 4.

Figure 4. TEM image of Ardisia crenata silver nanoparticle

2.5. *Antioxidant Activity*

2,2-diphenyl-1-picrylhydrazyl (DPPH Assay)

5µl of different stock of the test compound for Ardisia crenata (0-2500 µg/ml) and quercetin (0-50 µg/ml) was added to 0.1 ml of 0.1mM DPPH solution in a 96 well plate. The reaction was set in triplicate form and duplicates of blank was prepared containing 0.2 ml DMSO/Methanol and 5µl compound of different concentrations for Sample (0-2500 µg/ml) and for STD (0-50 µg/ml).The plate was incubated for 30 min in dark. At the end of the incubation, the decolorization was read at 495 nm using a micro plate reader (iMark, BioRad). Reaction mixture containing 20µl of deionized water was served as control. The scavenging activity was presented as '% inhibition' with respect to control [9].

2,2'-azino-bis(3-ethylbenzothiazoline-6-sulfonic acid) ABTS Radical Scavenging Activity

ABTS radicles were prepared by mixing APS (2.45 mM) and ABTS (7mM) solution, which was diluted 100X to prepare ABTS free radical reagent. Add 10µl of different stocks of the standard (Ascorbic Acid, 0-50 µg/ml) and sample (0 to 100 µg/ml) to 200µl of ABTS free radical reagent in a 96-well plate. Incubate at room temperature for 10 minutes in the dark. After incubation, the absorbance of the decolorization was measured at 750 nm using a microplate reader (iMark, BioRad). The results were presented with respect to the negative control [10].

2.6. *Cytotoxicity and Cell Viability*

3-(4,5-dimethylthiazol-2-yl)-2,5-diphenyltetrazolium bromide MTT Assay (MCF-7 Cell Lines)

The cytotoxicity of the provided samples against the MCF-7 cell line was assessed using the MTT Assay. Initially, cells were seeded at a density of 10,000 cells per well in a 96-well plate and cultured for 24 hours in DMEM medium supplemented with 10% FBS and 1% antibiotic solution at 37°C with 5% carbon di oxide CO2. Subsequently, the cells were treated with varying concentrations (ranging from 1 to 1000 µg/ml) of the formulations, which were prepared in incomplete medium. Following a 24-hour incubation period, MTT Solution at a final concentration of 250 µg/ml was added to the cell culture and further incubated for 2 hours. Upon completion of the incubation, the culture supernatant was aspirated, and the cell layer matrix was dissolved in 100 µl Dimethyl Sulfoxide (DMSO). The absorbance was then measured using an Elisa plate reader (iMark, Biorad, USA) at 540 nm and 660 nm wavelengths [11].

NRU Assay (THP-1 Cell Line)

Cytotoxicity of the provided samples on THP-1 cell line was determined by NRU Assay. The cells (5000-8000 cells/well) were cultured in 96 well plates for 24 h in DMEM medium (AT149- 1L) supplemented with 10% FBS (HIMEDIA-RM 10432) and 1% antibiotic solution at 37°C with 5% CO2. Next day, medium was removed and fresh culture medium was added to each well of the plate. 5 µl of treatment dilutions (of different concentrations) were added to the defined wells and treated plates were incubated for 24 h. 100 µl of NRU (40 µg/ml in PBS) was added to the defined wells and incubated (Heal Force-Smartcell CO2 Incubator-Hf-90) for 1 h. After that medium was removed, NRU was dissolved in 100 µl of NRU Destain solution. Finally plates were recorded at 550/660 nm [12].

MTT Assay (HepG2 cell line)

The cytotoxicity assessment of the provided samples against the HepG2 cell line was conducted using the MTT Assay. Initially, cells were seeded at a density of 10,000 cells per well in a 96-well plate and incubated for 24 hours in DMEM medium supplemented with 10% FBS and 1% antibiotic solution at 37°C with 5% CO2. The following day, cells were exposed to concentrations ranging from 1 to 1000 µg/ml of the formulations, prepared in incomplete medium. Following a 24-hour incubation period, MTT Solution at a final concentration of 250 µg/ml was added to the cell culture and incubated for an additional 2 hours. Upon completion of the incubation, the culture supernatant was aspirated, and the cell layer matrix was dissolved in 100 µl of Dimethyl Sulfoxide (DMSO). Subsequently, the absorbance was measured using an Elisa plate reader at 540 nm and 660 nm wavelengths [13].

3. Result and Discussion

The extraction process yielded a percentage extract of approximately 6.4%. The UV spectrum at 387 nm of the extract displayed absorption peaks corresponding to the presence of specific phytochemicals, such as flavonoids or phenolic compounds, known for their antioxidant properties. These compounds are likely responsible for the observed cytotoxic activity against cancer cell lines. The EPR spectrum provided additional information regarding the presence of free radicals or paramagnetic species within the extract, which could contribute to its biological activity.

3.1 Characterization of Optimized Ardisia crenata Silver Nanoparticles

FT-IR of Ardisia crenata

At a wave number of 3219.5 cm-1, the observed vibration indicating O-H stretching suggests the presence of hydroxyl (OH) groups, commonly associated with alcohols, phenols, and carboxylic acids. The wave number 3095.88 cm-1 corresponds to N-H stretching, indicative of amino (NH) groups typically found in amines, amides, and proteins. Additionally, the presence of aliphatic C-H bonds, prevalent in alkanes and alkyl groups, is suggested by the wave number 2954 cm-1. The wave number 1537 cm-1 corresponds to the C=O stretching vibration, characteristic of the carbonyl (C=O) functional group present in various compounds such as aldehydes, ketones, carboxylic acids, and esters. Lastly, the wave number 1211 cm-1 corresponds to both C-C and C-N stretching vibrations, indicative of carbon-carbon (C-C) bonds typically found in aromatic rings, and carbon-nitrogen (C-N) bonds commonly present in amines, respectively as shown in fig. 5 and in table 1.

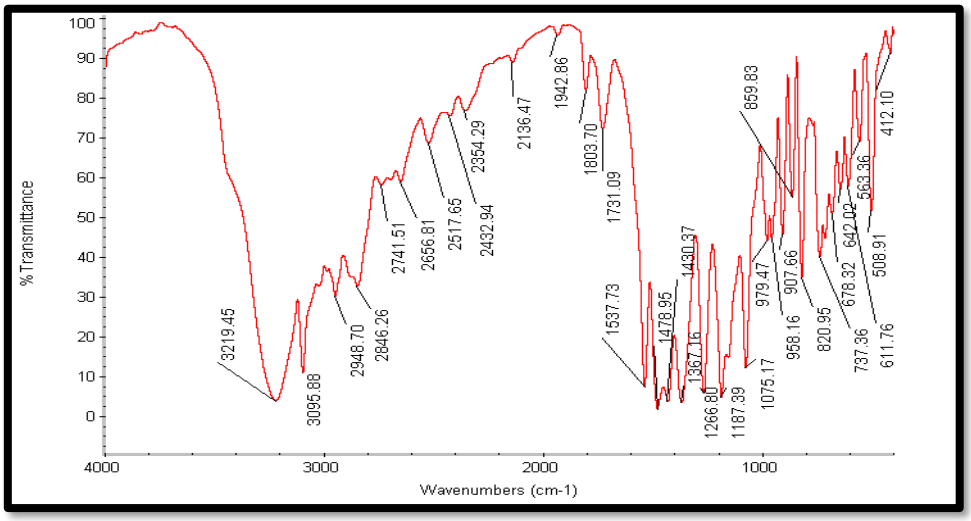

Figure 5. FT-IR Spectrum of *Ardisia crenata*

Table 1. Interpretation of FT-IR Spectrum of *Ardisia crenata*

Wave Number	Interpretation
3219.5	O-H Stretching[17]
3095.8	N-H Stretching[17]
2948	C-H Stretching (aliphatic)[17]
1731	C=O Stretching[17]
1266	C-C and C-N Stretching[17]

FT- IR of Ardisia crenata silver nanoparticle

At 3219.5 cm-1, the observed O-H stretching vibration signifies the presence of hydroxyl (OH) groups, prevalent in alcohols, phenols, and carboxylic acids. The wave number 2947 cm-1 corresponds to the C-H stretching vibration characteristic of aliphatic compounds, such as alkanes and alkyl groups, featuring prevalent carbon-hydrogen (C-H) bonds. Observed at 1537 cm-1, the C=O stretching vibration indicates the presence of the carbonyl (C=O) functional group, commonly encountered in compounds like aldehydes, ketones, carboxylic acids, and esters. The wave number 1267 cm-1 corresponds to both C-C and C-N stretching vibrations, with C-C stretching typically associated with aromatic rings and C-N stretching characteristic of amines. Finally, at 1074 cm^-1, the observed C-O-C stretching vibration suggests the existence of carbon-oxygen-carbon (C-O-C) bonds, commonly found in ethers, esters, and various organic compounds as shown in fig. 6 and table 2.

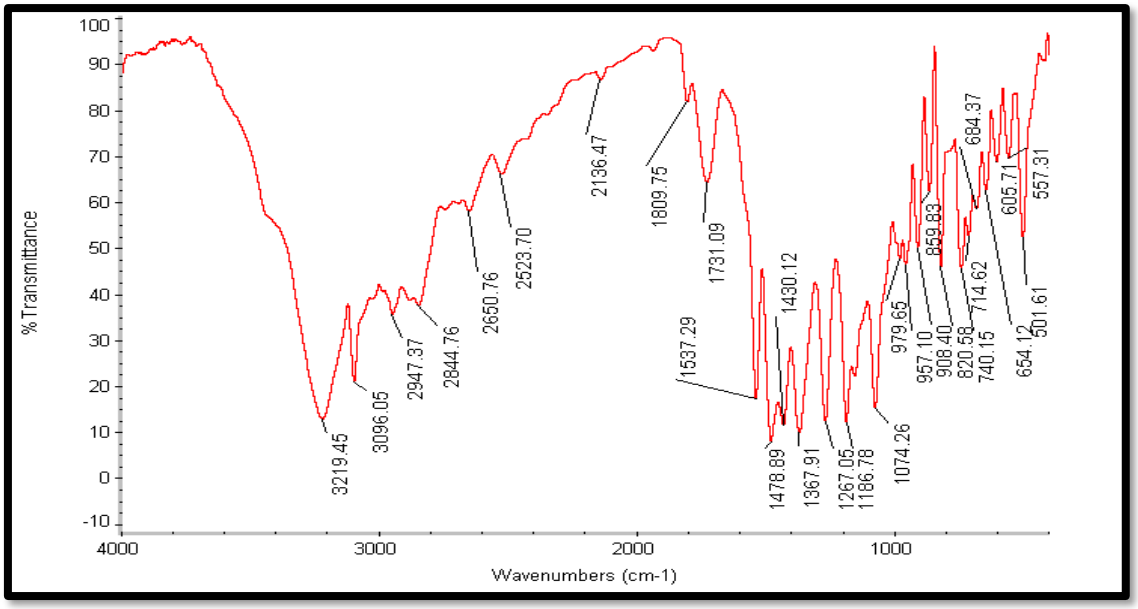

Figure 6. FT-IR Spectrum of *Ardisia crenata* silver nanoparticle

Table 2. Interpretation of FT-IR Spectrum of *Ardisia crenata* silver nanoparticle

Wave Number	Interpretation
3219.5	O-H Stretching[17]
2947	C-H Stretching (aliphatic)[17]
1537	C=O Stretching[17]
1267	C-C and C-N Stretching[17]
1074	C-O-C stretching[17]

3.2. XRD Analysis

X-ray diffraction (XRD) analysis was employed to investigate the molecular structure and polymorphism of polymeric nanoparticles in this study. The XRD patterns of pure Ardisia crenata, Blank nanoparticles, and the Ardisia crenata silver nanoparticles formulation are depicted in Fig. 7 and 8 respectively.

The XRD pattern of pure Ardisia crenata, ranging from 2 to 70° 2θ, exhibited distinctive peaks at approximately 12.7, 13.2, 18.5, 26.9, and 28 degrees. These peaks closely matched those of crystalline

Ardisia crenata, indicating its crystalline nature. In contrast, the XRD pattern of Blank nanoparticles did not display any high-intensity peaks, suggesting the amorphous nature of the polymer and stabilizer components. Notably, the characteristic peaks of Ardisia crenata were absent in the XRD pattern of Ardisia crenata silver nanoparticles. This absence indicates that Ardisia crenata was molecularly dispersed within the silver nanoparticles, and there may be minimal or no free drug present in a crystalline form on the surface of the nanoparticles, as illustrated in Fig. 4 and 5. These findings suggest effective encapsulation of Ardisia crenata within the matrix of the nanoparticles and potentially enhancing its stability and bioavailability for therapeutic applications.

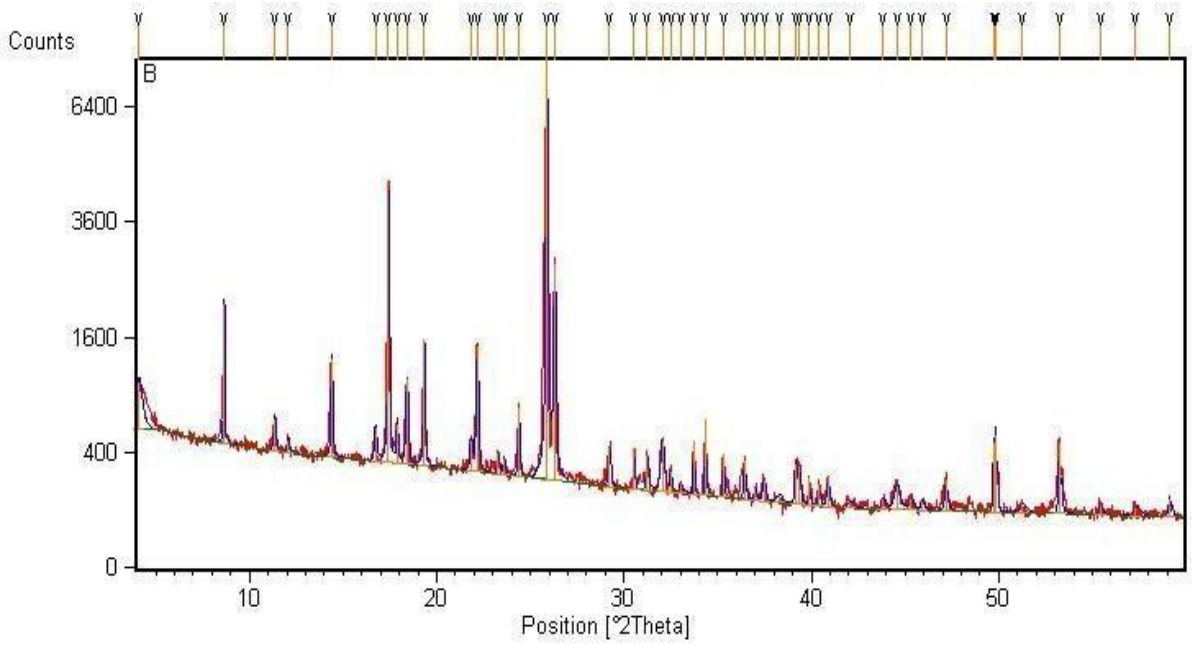

Figure 7. XRD pattern of Ardisia crenata

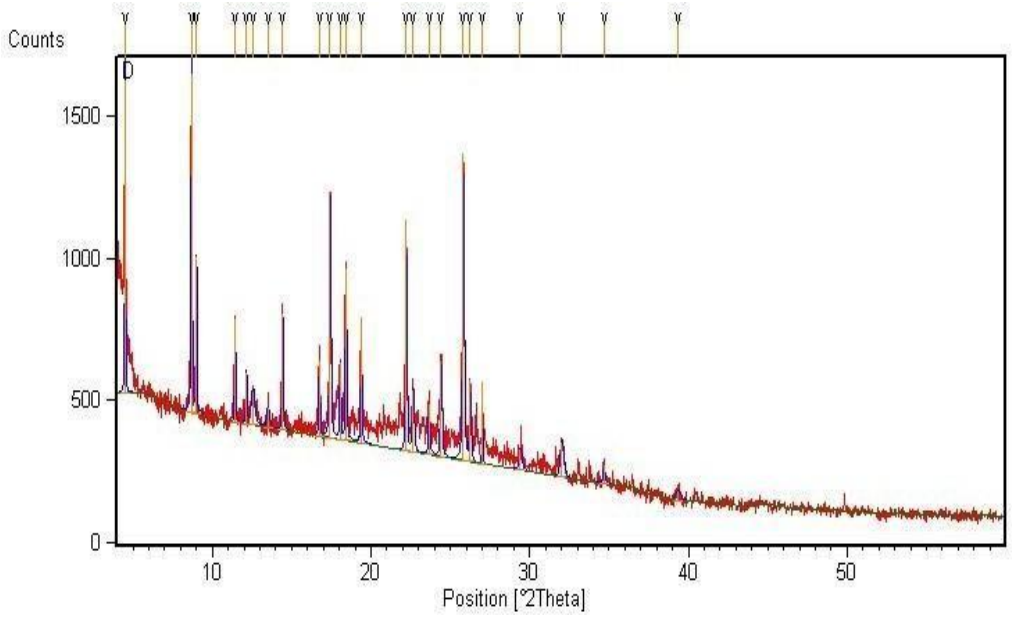

Figure 8. XRD pattern of *Ardisia crenata* Nanoparticle

3.3 Antioxidant Activity

2,2-diphenyl-1-picrylhydrazyl (DPPH Assay)

The DPPH scavenging activity assay evaluates the capacity of compounds to counteract free radicals by providing hydrogen atoms or electrons, thereby converting the DPPH radical to its non-radical form. The percentage of DPPH scavenging activity serves as a metric for the efficiency of the sample in neutralizing these radicals. In the dataset provided, ascorbic acid demonstrates an IC50 value of 25.99 µg/ml, signifying that it achieves 50% DPPH scavenging activity at this concentration. Conversely, Ardisia crenata silver nanoparticle exhibits a lower IC50 value of 12.2 µg/ml, indicating its ability to achieve the same scavenging activity at a reduced concentration. This suggests that Ardisia crenata silver nanoparticle possesses a higher antioxidant potency than ascorbic acid, requiring a smaller concentration to neutralize 50% of DPPH radicals. Lower IC50 values denote heightened antioxidant potential, implying superior efficacy in shielding cells from oxidative harm. Consequently, based on the provided data, Ardisia crenata silver nanoparticle displays superior antioxidant activity compared to ascorbic acid, showcasing its potential as a potent antioxidant agent shown in table 3 and fig. 9 and 10 [14]

DPPH Scavenging activity = ((Abs Control- Abs Sample)/Abs Control) ×100

Table 3. DPPH Assay

Sample code	IC_{50} value (µg/ml)
Ascorbic Acid	25.99
Ardisia crenata Silver Nanoparticle	12.2

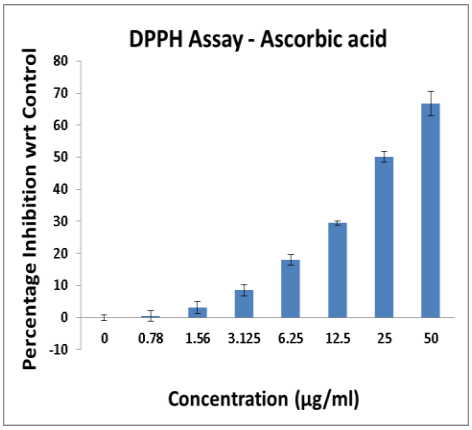

Figure 9. DPPH Assay- Ascorbic Acid

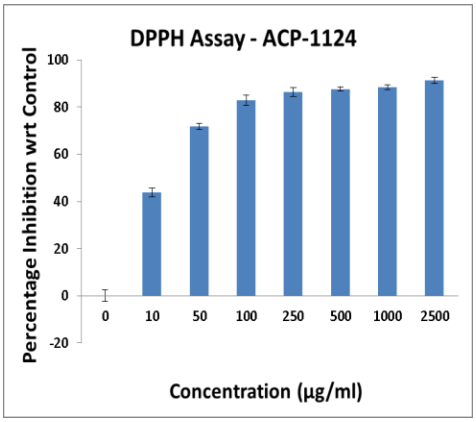

Figure 10. DPPH Assay

2,2'-azino-bis(3-ethylbenzothiazoline-6-sulfonic acid) (ABTS Radical Scavenging Activity) Ardisia crenata silver nanoparticle exhibits an IC50 value of 3.781 µg/ml, while ascorbic acid has an IC50 value of 1.164 µg/ml in the DPPH scavenging activity assay. These IC50 values indicate the concentration at which each sample achieves 50% DPPH scavenging activity.

A lower IC50 value signifies that a smaller concentration of the sample is required to neutralize 50% of the DPPH radicals, indicating stronger antioxidant potency.

Thus, based on the result, ascorbic acid exhibits superior antioxidant activity over Ardisia crenata silver nanoparticles in terms of its ability to scavenge DPPH radicals effectively at a lower concentration shown in table 7 and fig. 11 and 12 [17,18,19].

Table 4. ABTS Radical Scavenging Activity

Sample code	IC_{50} value (µg/ml)
Ardisia crenata Silver Nanoparticle	3.781
Ascorbic Acid	1.164

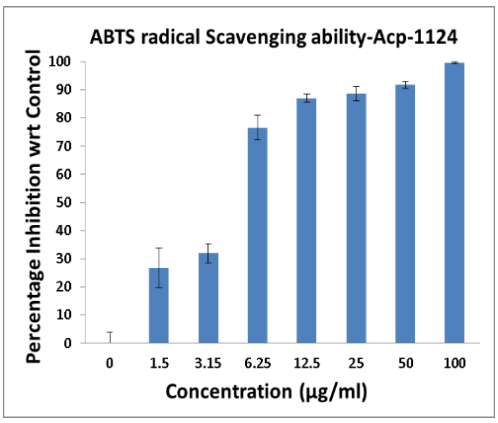

Figure 11. ABTS Radical Scavenging ability

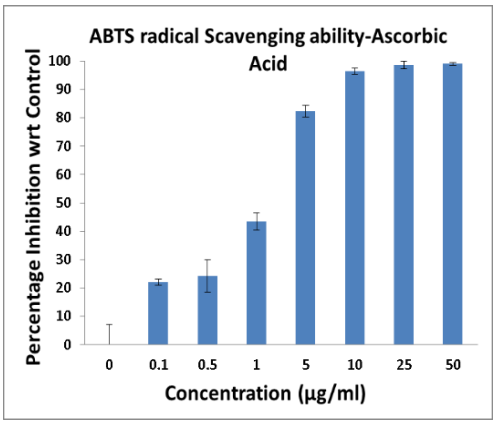

Figure 12. ABTS radical Scavenging ability Ascorbic acid

3.4. Cytotoxicity and Cell Viability

MTT Assay (MCF-7 Cell Lines)

The IC50 value of Ardisia crenata for the MCF-7 cell line was determined to be 753.4 µg/ml. This value represents the concentration required to inhibit the growth of MCF-7 cancer cells by 50% in vitro. The relatively high IC50 value suggests that a significant concentration of the compound is needed to exert cytotoxic effects against MCF-7 cells. However, it's essential to consider that Ardisia crenata may exhibit cytotoxicity against MCF-7 cells at higher concentrations, as depicted in Table 5.

Table 5. Assay (MCF-7-Cell Lines

Sample code	IC50 value (µg/ml)
Ardisia crenata	753.4

NRU Assay (THP-1 Cell Line)

The IC50 value of Ardisia crenata for the THP-1 cell line is 15.06 µg/ml. This IC50 value represents the concentration of Ardisia crenata required to inhibit cell viability by 50% in vitro, as assessed by the Neutral Red Uptake (NRU) assay. A lower IC50 value indicates that a smaller concentration of the sample is needed to induce cytotoxic effects, leading to a 50% reduction in cell viability. In this case, the relatively low IC50 value of 15.06 µg/ml for Ardisia crenata suggests that the compound exhibits significant cytotoxicity against THP-1 cells at relatively low concentrations. The result implies that Ardisia crenata has potential as a cytotoxic agent against THP-1 cells in vitro shown in table 6 [15].

Table 6. NRU Assay (THP-1-Cell Line)

Sample code	IC50 value (µg/ml)
Ardisia crenata	15.06

MTT Assay (HepG2 cell line)

The IC50 value of Ardisia crenata for the HepG2 cell line is 324.8 µg/ml. This IC50 value represents the concentration of Ardisia crenata required to inhibit cell viability by 50% in vitro, as determined by the assay performed using HepG2 cells. The IC50 value is an important indicator of the compound's potency in exerting cytotoxic effects on the tested cells. In this case, the relatively high IC50 value of 324.8 µg/ml suggests that a considerable concentration of Ardisia crenata is needed to achieve a 50% reduction in cell viability in HepG2 cells shown in table 7 [16].

Table 7. MTT Assay (HepG2 cell line)

Sample code	IC50 value (µg/ml)
Ardisia crenata Silver Nanoparticles	324.8

4. Conclusion

Our study highlights the cytotoxic properties of *Ardisia crenata* across diverse cell lines, revealing variable responses as reflected by distinct IC50 values. The compound exhibited weak cytotoxicity in the MCF-7 cell line (IC50: 753.4 µg/ml), moderate activity in the HepG2 cell line (IC50: 324.8 µg/ml), and potent efficacy against the THP-1 leukemia cell line (IC50: 15.06 µg/ml). These findings emphasize the importance of evaluating cytotoxic effects across multiple cell lines due to variability in cellular responses. While *Ardisia crenata* demonstrates promise, further research is needed to elucidate its mechanism of action, assess selectivity, and explore its pharmacokinetic and in vivo efficacy. This work establishes a foundation for advancing *Ardisia crenata* as a potential anticancer agent, contributing to the development of novel therapeutic strategies.

Acknowledgement

The author gratefully acknowledges the support of, Faculty of Pharmacy, Veer Bahadur Singh Purvanchal University, for providing necessary facilities to carry out this research work.

Conflicts of Interest

The authors declare no conflict of interest.

References

1. Khan MA, Khan T, Adil SF, et al, 2017. Green synthesis of silver nanoparticles mediated by Pulicaria glutinosa extract. Int J Nanomed. 12, Pages-275-284.
2. Saxena VK, Mishra G, Islam A, et al, 2017. A review on phytochemical and pharmacological aspects of Ardisia crenata Sims. Res. J. Phytochem. 11(1), Pages- 26–34.
3. Singh P, Kim YJ, Zhang D, Yang DC. 2016. Biological synthesis of nanoparticles from plants and microorganisms. Trends Biotechnol. 34(7), Pages-588–599.
4. Narmani A, Ahmadi M, Rahmani F, et al, 2019. Nanoparticles in cancer treatment: Opportunities and challenges. Pharm. Nanotechnol. 7(3), Pages-178–185.
5. Zainal Abidin N, Othman HH, Syahirah AA, et al. 2020. Cytotoxicity evaluation of hydroethanolic extracts of Tamarindus indica seed and pulp on MCF-7 human breast cancer cells. BMC Complement Med. Ther. 20(1), Pages- 197.
6. Uthra C, Sivagnanam UTH, Manoj Kumar A, et al. 2020. Cytotoxic activity of methanol extract of Tabernaemontana heyneana Wall. ex G. Don leaves against human cancer cell lines. J. Tradit. Complement. Med. 10(4), Pages-350–355.
7. Hossain MM, Ali MS, Saha A, et al. 2019. Evaluation of cytotoxic activity of three wild edible mushrooms from northeast India against human cancer cell lines. Biomed. Pharmacother, 109, Pages-1239–1245.
8. Hasan MM, Alam MJ, Islam MJ, et al. 2021. Antioxidant and cytotoxic activities of different extracts of Spilanthes paniculata whole plant. J. Tradit. Complement. Med., 11(4), Pages-358–363.
9. Emami SA, Abedindo B, Bagheri AH, et al. 2019. Cytotoxic activity of some medicinal plant extracts from Mazandaran province, Iran. Avicenna J. Phytomed. 9(3), Pages-252–259.
10. Khan I, Rahman H, Khan TA, et al. 2020. Phytochemical analysis, antioxidant and cytotoxic

activity of methanolic extract of Fagonia indica. Bangladesh J. Pharmacol. 15(3), pages-188–193.
11. Panda D, Pattnaik S, Nayak BS, et al. 2019. Antioxidant, cytotoxicity, and apoptosis induction studies of β-sitosterol-3-O-glucopyranoside isolated from Allium cepa. Asian Pac. J. Trop. Med. 12(1), Pages- 41–47.
12. Mahomoodally MF, Soobrattee MA, Renugadevi N, et al. 2019. Evaluation of cytotoxicity and antioxidant activity of extracts from Mauritian endemic plants in human cancer cell lines. J. Ayurveda Integr. Med. 10(4), Pages-253–261.
13. Lima ES, Santos SA, Oliveira WDA, et al. 2020. Evaluation of cytotoxic, genotoxic, and antioxidant activities of Helicteres sacarolha A. St. Hill. J. Toxicol. Environ. Health Sci. 12(4), Pages- 75–85.
14. El-Seedi HR, Moustafa MF, Khalifa SA, et al. 2021. Cytotoxic, anti-inflammatory, and antioxidant activities of Rubia tinctorum L. root extract and its major compounds. Nat. Prod. Res. 35(10), Pages-1781–1785.
15. Madje BR, Chavan MJ, Kanawade VD, et al. 2019. Evaluation of cytotoxicity and apoptosis induction by Eupatorium triplinerve Vahl. root extract in human colon cancer HT-29 cells. J. Ethnopharmacol. 235, Pages-328–334.
16. Kaviya S, Santhanalakshmi J, Viswanathan B, et al, 2018. Green synthesis of silver nanoparticles using Polyalthia longifolia leaf extract along with D-sorbitol: Antibacterial activity against Staphylococcus aureus and Escherichia coli. Microbial Pathogenesis, 121, 184–188.
17. Silverstein RM, Webster FX, Kiemle DJ. 2005. Spectrometric Identification of Organic Compounds (7th ed.). John Wiley & Sons, 71–143.
18. Saxena P., Singh N., and Singh SK., Ardisia Crenata: A New Source of Health-Promoting Phytopharmaceuticals and Chemicals. (2022). *Journal of Pharmaceutical Negative Results*, 4907-4914. https://doi.org/10.47750/pnr.2022.13.S10.595
19. Singh SK., Singh N., and Saxena P., Therapeutic Nanoparticles: A Promising Drug Delivery System. (2022). *Journal of Pharmaceutical Negative Results*, 4915-4927. https://doi.org/10.47750/pnr.2022.13.S10.596